Can. Aeronaut. Space J., Vol. 57, No. 1, pp. 59–64, 2011

Virtual soil calibration for wheel–soil interaction simulations using the discrete-element method

R. Briend, P. Radziszewski, and D. Pasini

Abstract. Lunar mobility studies require a precise knowledge of the geotechnical properties of the lunar soil when it comes to design-adapted and efficient-traction systems. The remarkable progress of computers since the Apollo missions allows direct testing of the performance of new design prototypes through simulations of soil-structure interactions using the discrete-element method (DEM). Before simulating traction-system displacements on the soil, the virtual-soil parameters need to be calibrated. This study presents a systematic method for calibrating a granular soil through four steps: (1) measurement of three of the real-material properties through two experiments, (2) determination of the design variables defining the virtual soil, (3) construction of surrogate models for the virtual-material properties as a function of the design variables via simulated experiments, and (4) optimization of the design-variable values to fit the virtual-soil properties to the real-soil values. Two different experiments, a direct-shear test and an angle-of-repose measurement, were used to determine the following material properties: cohesion, internal angle of friction, and angle of repose. Optimum DEM parameters were computed to characterize two types of soil: silica sand, based on an experimental direct-shear test and angle-of-repose measurements, and lunar regolith, based on data from the literature.

Résumé. Les études de mobilité sur le sol lunaire requièrent une connaissance précise des propriétés géotechniques du sol lunaire lorsqu'il est question de systèmes adaptés et efficaces de traction. Les progrès remarquables réalisés dans le domaine de l'informatique depuis les missions d'Apollo permettent de tester directement les performances des nouveaux modèles de prototypes par le biais de la simulation des interactions sol-structure à l'aide de la méthode des éléments discrets (DEM). Avant de pouvoir simuler les déplacements d'un système de traction, les paramètres du sol virtuel doivent être étalonnés. Dans cette étude, on présente une méthode systématique pour l'étalonnage d'un sol granuleux en quatre étapes: (1) la mesure de deux des propriétés réelles des matériaux au moyen de trois expériences, (2) la détermination des variables du concept définissant le sol virtuel, (3) la construction de modèles de substitution pour les propriétés matérielles virtuelles en fonction des variables du concept en effectuant des expériences de simulation et (4) l'optimisation des valeurs des variables du concept pour ajuster les propriétés virtuelles du sol aux valeurs réelles du sol. Deux expériences différentes, l'essai de cisaillement direct et la mesure de l'angle de repos, sont effectuées pour déterminer les propriétés matérielles suivantes: la cohésion, l'angle de frottement interne et l'angle de repos. Les paramètres DEM optimum sont calculés pour caractériser deux types de sol: la sable siliceux, à partir des mesures expérimentales du test de cisaillement direct et des mesures de l'angle de repos et, le régolite lunaire, à partir des données puisées dans la littérature.

Nomenclature

c	cohesion of a soil
φ	internal angle of friction of a soil
A	angle of repose of a soil
ρ	density of a material
v	Poisson's ratio for a material
G	shear modulus of a material
μ_s	static-friction coefficient of aninteraction
μ_r	rolling-friction coefficient of an interaction
e	restitution coefficient of an interaction
r	mean particle radius
ϕ_i	objective function i

Introduction

Designing efficient and terrain-adapted wheels requires accurate modelling of the wheel–soil interaction. The discrete-element method (DEM) is the appropriate way to simulate these interactions if the wheel is intended for use on granular soils. Indeed, the DEM can accurately model granular materials as an assembly of distinct particles and can precisely compute its interaction with solid geometries. The behaviour of a virtual material modelled with DEM software depends on the parameters used to characterize it. Consequently, the fine calibration of these parameters is a prerequisite step in any realistic DEM simulation. A calibration method was published by Coetzee and Els (2009). They used two-dimensional DEM simulations to model the behaviour of corn seeds during a silo discharge. The virtual particles' stiffness was first calibrated through a

Received 6 December 2010. Accepted 6 April 2011. Published on the Web at http://pubs.casi.ca/journal/casj on 14 December 2011.

R. Briend, P. Radziszewski[1], and D. Pasini, Department of Mechanical Engineering, McGill University, Montréal, QC H3A 2K6, Canada.

[1]Corresponding author (e-mail: peter.radziszewski@mcgill.ca).

compression test. Then the friction coefficient was tuned through a shear test. These two experiments revealed a couple of unique parameter values for which the virtual-soil properties matched the real-soil values.

The present study describes a calibration methodology developed to model lunar regolith for the design of a lunar-rover wheel. This methodology is innovative in three respects. First, it involves three-dimensional DEM simulations, using the EDEM software. Second, it identifies the parameters with the greatest impact on virtual-soil properties among the set of particle-design variables. Third, it finds the optimum values for these parameters to minimize the overall error between the virtual- and real-soil properties, even if the objectives of matching each soil property separately are conflicting.

This methodology consists of four steps. First, three of the real material properties are measured through two geotechnical experiments (“Direct shear test and angle-of-repose experiment” section). Then the design variables describing a virtual soil in EDEM are identified and the variables with the greatest impact on the soil properties are listed through a screening experiment (“Determination of the design variables of the virtual soil” section). Next, surrogate models are computed from simulations of the geotechnical experiments to describe the response surface of the virtual soil as a function of its design variables (“Construction of surrogate models for the properties of the virtual soil” section). Finally, an optimum set of design variables is found that minimizes the gap between the virtual soil’s properties and the real-soil values (“Optimization” section).

Direct-shear test and angle-of-repose experiment

To characterize the real soil, experiments that would yield soil properties relevant to our study were modelled. These included the displacement of a traction system on a deformable soil — simple to model with our DEM software — to build the virtual soil’s response surface (cf. “Construction of surrogate models for the properties of the virtual soil” section).

The direct-shear test meets these criteria, as its experimental setup consists of only three parts and it allows both the soil’s cohesion, c, and the internal angle of friction, φ, to be determined. These two properties give the soil’s maximum shear stress, τ_{max}, through the Mohr Coulomb law

$$\tau_{max} = c + p \tan \varphi \quad (1)$$

where p is the pressure in the soil (Bekker, 2008). The maximum shear stress is important, as it determines the maximum thrust of a wheel or a track on the soil. The setup of the direct-shear test consists of a three-part box filled with the granular material to be studied (**Figure 1**). A constant load is applied on the top part so that the soil specimen is subjected to a constant pressure, p. The bottom frame of the box remains stationary while an increasing longitudinal force, F, applied on the upper frame makes it glide on the bottom frame. The longitudinal force (F) and the displacement of the upper frame relative to the bottom frame are recorded. As the contact between the two frames is frictionless, F is then the shear force and is equal to the shear stress multiplied by the cross-sectional area of the box, S: $F = S \times \tau$. F ultimately reaches a threshold, which corresponds to the shear failure of the soil on the plane between the two frames: $\tau_{max} = F_{max}/S$. This experiment is run under various pressures (p) by applying different normal loads to the top part of the box, and the linear regression of the maximum shear stresses, τ_{max}, plotted with respect to p gives the soil cohesion, c, and internal angle of friction, φ, according to the Mohr Coulomb law (Equation 1).

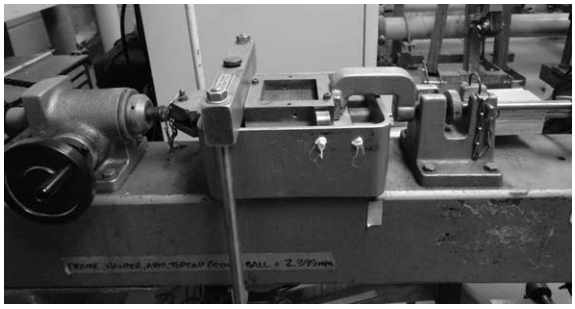

Figure 1. Direct shear test experiment setup (British Standards Institution BS 1377-1 1990).

The second experiment used for our calibration study was the angle-of-repose experiment. The low cohesion and high deformability of granular soils induce an important phenomenon on the wheel soil interaction. Indeed, since a wheel rolling on a granular soil tends to sink, the resistance to motion of the soil on the wheel depends on how the soil is moved by the front of the wheel and how the soil will recover the side faces. This avalanching process occurring in a sloping soil can be illustrated by the angle-of-repose experiment. The angle of repose, A, of a granular material is one of its most distinctive properties; it imposes shape on a heap of gravel or a sand dune, for instance. However, it is not an intrinsic property of the material and can depend on the experimental conditions. Different experimental setups can be used to measure it, the most common being the slow lifting of a vertical tube filled with material and initially laying the material on a plate, or the lifting of one side of a filled box. We chose the tube setup, as it was used by Ji and Shen (2009) in their two-dimensional DEM angle-of-repose simulations. We extended their study to three-dimensional simulations in order to build the surrogate model of the angle of repose of the virtual soil (“Sensitivity analysis” section).

To conclude, the three material properties used in this virtual soil calibration process are cohesion and internal angle of friction (determined with the direct-shear test) and angle of repose. **Table 1** gives the values of these properties

for a silica Barco sand (measured by N. Kaveh-Moghaddam) and lunar regolith (Heiken, 1991).

Determination of the design variables of the virtual soil

The following section describes how a virtual soil is modelled in EDEM and how the important design variables describing the virtual soil are identified through a sensitivity analysis.

Soil modeling with EDEM

The DEM software EDEM models granular soils from predefined "particle prototypes" and particle-creation rules, called factories (EDEM, 2009). It computes the interactions between the granular material and rigid geometries built from simple polygons through EDEM's graphical user interface, or imported from CAD models. A particle prototype consists of a sphere or a union of spheres, each characterized by its radius, r, and center position. Consequently, a granular material made up of nonspherical particles (corn seeds, for example) can be modelled by a particle prototype, including several spheres. The particle-creation rules (EDEM, 2009), or factories, define how the particle should be created. The main parameters characterizing a factory are the number of particles to be created, time and place of creation, particle prototype, and size distribution. Each particle prototype or other geometric element used in a simulation is associated with a material, with density ρ, Poisson's ratio υ, and shear modulus G. The contact model used to compute the interaction forces between two contacting spheres that belong to two different particles is detailed in *EDEM's User guide* (EDEM, 2009) and is based on the Hertz Mindlin model (Mindlin, 1949; Tanaka et al., 1992). It characterizes the interactions by means of three coefficients: restitution, e, static friction, μ_s, and rolling friction, μ_r. The coefficient of rolling friction, which is specific to EDEM, models the effect of surface roughness on nonspherical particles. Indeed, as the virtual particles are made up of spheres, they can roll on each other without friction. To avoid this artificial feature, the rolling-friction coefficient introduces an artificial torque in the contact model opposed to this rolling motion.

Table 1. Lunar regolith and silica Barco sand properties: cohesion, internal angle of friction, and angle of repose.

	Lunar regolith	Silica Barco sand
c	0.1–1 kPa	0.024 kPa
φ	30°–50°	26.6°
A	65°	30°

Sensitivity analysis

In this study, a unique spherical-particle prototype was used. Indeed, it was shown that the macroscopic behaviour of virtual soils made up of spherical or nonspherical particles can be similar, provided that the rolling-friction coefficient is precisely tuned (Briend, 2010). As explained in the previous section, this particle prototype is characterized by the following parameters: r, ρ, ν, G, μ_s, μ_r, and e. A screening experiment was conducted to identify which parameters have a strong impact on the properties of the virtual soil and which others can be neglected in the calibration process so as to reduce the simulation run time and model complexity. The screening experiment chosen was the angle-of-repose experiment. The experimental setup was a three-dimensional extension of Ji and Shen's (2009) two-dimensional DEM angle-of-repose simulations: a 1.5 mm diameter steel tube containing 3000 particles initially rests vertically on a plate and is then lifted upwards at a speed of 5 mm/s (**Figure 2**). When the particle pile reaches a static state, which occurs around $t = 0.7$ s, the particle positions are stored in a table and the angle of repose of the pile is computed with a MATLAB function. The simulation run time was approximately 2 h on a 8-core 3 GHz workstation.

First, five simulations were analysed with an initial set of parameters close to the regolith values ($r = 50$ μm, $\rho = 3000$ kg/m^3, $\nu = 0.2$, $G = 5 \times 10^7$ Pa, $\mu_s = 0.3$, $\mu_r = 0.1$, $e = 0.5$) (Heiken, 1991), which gave an average angle of repose of 27.47° (standard deviation = 0.52°). Then one parameter was changed successively while keeping the other six at their initial values, and the average angle was computed (**Table 2**). **Table 2** shows that the angle of repose depends mostly on the coefficients of static and rolling friction, and to a lesser extent on the mean particle radius. Indeed, their sensitivity derivatives, expressed as the variation in the angle of repose ($\Delta A/A$) over the parameter variation considered ($\Delta P/P$), have the greater absolute values. As a consequence, these three parameters (r, μ_s, μ_r) were regarded as the design variables of our virtual soil, and the response surface for the soil properties was built as a function of them.

Construction of surrogate models for the properties of the virtual soil

In this section, surrogate models describing the response surface of the virtual soil are built as a function of its design variables (r, μ_s, μ_r) for each of the following properties, cohesion, internal angle of friction, and angle of repose, by simulating the direct-shear test and the angle-of-repose experiment for different sets of design variables. The angle-of-repose simulation is described in the "Sensitivity analysis" section above. Let us briefly describe the direct shear test simulation. To simulate this experiment within an acceptable time (i.e., a few hours), we modelled only a slice of the box used in the experimental setup, setting periodic boundaries

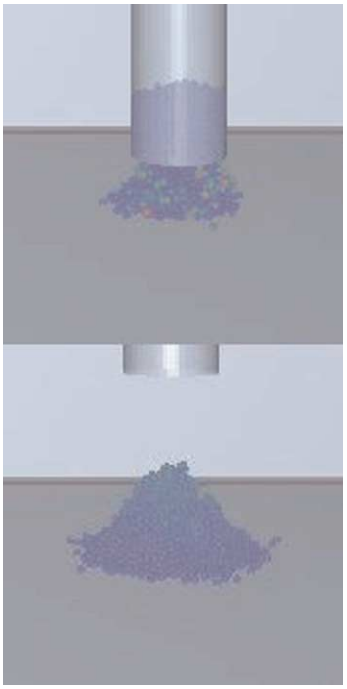

Figure 2. Angle-of-repose simulation; the tube is lifted (top) until the virtual soil remains motionless on the plate (bottom).

on both sides of the slice (**Figure 3**). The slice width was set to five times the mean particle radius to ensure that a particle had no chance of interacting with itself because of the periodic boundaries. In our simulations, the upper frame remained stationary while a translation of constant velocity was imposed on the lower frame (**Figure 3**). A plane macroparticle subject to a constant vertical force applied the desired pressure on the soil. The horizontal component, F_x, of the total force of the soil on the lower frame was recorded. **Figure 4** shows the force F_x plotted with respect to time for different pressures. F_x reaches a plateau after approximately 0.2 s, which allows us to compute the maximum shear stress $\tau_{max} = F_{max}/S$. Cohesion and internal angle of friction were then computed with the linear regression of τ_{max} with respect to the pressure, p (Equation 1).

Table 2. Angle-of-repose measurement after modification of one parameter in the initial set.

Value of modified parameter	A (avg. of three simulations), deg.	SD (deg.)	Sensitivity derivative (absolute value), %
$r = 100$ μm	26.37	0.53	4.0
$\rho = 4000$ kg/m^3	27.67	0.34	2.2
$v = 0.4$	27.95	0.28	1.7
$G = 7 \times 10^7$ Pa	27.06	0.44	3.7
$\mu_s = 0.5$	31.48	0.64	21.9
$\mu_r = 0.2$	36.57	0.76	33.1
$e = 0.3$	27.63	0.61	0.8
Initial set	27.47	0.52	

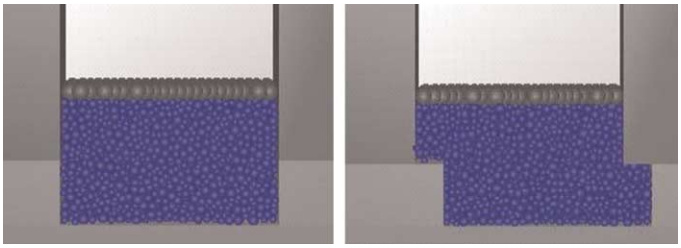

Figure 3. Direct shear test box before and after translation of the lower frame.

Design of the experiment

As EDEM software does not allow code programming, each new simulation has to be set manually through the graphical user interface. This prevents any automated update of the surrogate models in order to refine them in a given design region. For this reason, our surrogate models need to be accurate in the whole design space. The following experimental design was chosen: simulations were run for each set of design variables ($r = r_0 = 50$ μm, μ_s, μ_r) with

$$\{\mu_s, \mu_r\} \in \{0; 0.1; 0.3; 0.5; 0.9; 1.3; 1.7\} \times \{0; 0.05; 0.1; 0.2; 0.3\}$$

For the purposes of illustration, **Figure 5** shows the angle-of-repose measurements for these design-variable sets. Thehe less important effect of r was then investigated by testing different particle radii ($r = 25$, 50, 100 200, 500 μm) with constant couples (μ_s, μ_r).

Second-order fit

Each surrogate model of the soil's properties c, φ, and A was then built as a product of two independent functions: $f(r = r_0, \mu_s, \mu_r)$, describing the response surface for $r = r_0 = 50$ μm, and $g(r)$, a dimensionless function of r. The function f was computed as the second-order fit of the data points because this fitting technique is simple and adapted

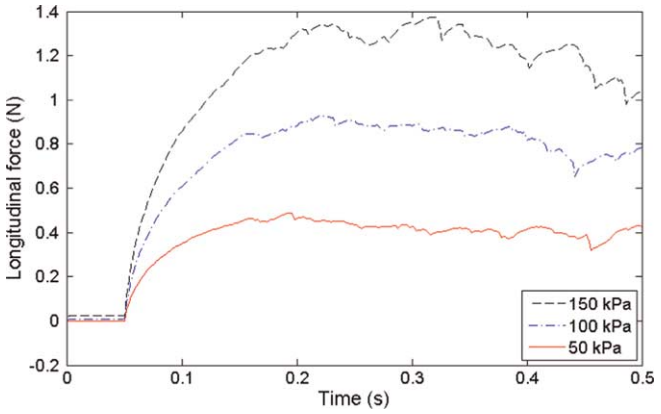

Figure 4. F_x with respect to time under various pressures, for ($r = 50$ μm, $\mu_s = 0.3$, $\mu_r = 0$).

to a curved response (Myers and Montgomery, 2002). For instance, the surrogate model of cohesion can be expressed as

$$c(r,\mu_s,\mu_r) = f_c(\mu_s,\mu_r)\cdot g_c(r), \quad \text{with } f_c = \left(\sum_{i+j\leq 2} c_{ij}\mu_s^i\mu_r^j\right) \tag{2}$$

in which the c_{ij} values are the components of the second-order fit, f_c. The final expression of the surrogate models computed from the simulation results and used in the following optimization section are

$$\begin{aligned} c(r,\mu_s,\mu_r) &= \left(4.17 + 39.30\mu_r - 18.04\mu_s + 30.14\mu_r^2 + 2.38\mu_s^2 + 52.55\mu_r\mu_s\right).\left(0.27 + \frac{r}{r_0} - 0.27\frac{r^2}{r_0^2}\right) \\ \varphi(r,\mu_s,\mu_r) &= \left(14.61 - 76.10\mu_r + 57.15\mu_s - 25.30\mu_r^2 - 25.57\mu_s^2 + 24.79\mu_r\mu_s\right).\left(0.71 + 0.44\frac{r}{r_0} - 0.15\frac{r^2}{r_0^2}\right) \\ A(r,\mu_s,\mu_r) &= \left(5.05 + 95.55\mu_r + 36.69\mu_s - 181.1\mu_r^2 - 18.98\mu_s^2 + 42.09\mu_r\mu_s\right).\left[1 - 0.1151n\left(\frac{r}{r_0}\right)\right] \end{aligned} \tag{3}$$

Optimization

As mentioned previously, our goal is to optimize the design variables of our virtual soil so that its properties (c, φ, A) would fit the real soil values (c_0, φ_0, A_0). Let us, then, define three objective functions, to be minimized as follows:

$$\phi_1(x) = \left|\frac{A(x) - A_0}{A_0}\right| \quad \phi_2(x) = \left|\frac{c(x) - c_0}{c_0}\right| \quad \phi_3(x) = \left|\frac{\varphi(x) - \varphi_0}{\varphi_0}\right|$$

in which the set of design variables is written as $x = (r, \mu_s, \mu_r)$ for the sake of clarity. Moreover, let us build a fourth objective function, $\phi_4 = \phi_4(r)$, a function of the mean particle radius only, positive and decreasing towards zero when r increases. The purpose of this objective function is to illustrate the preference for larger particles. Indeed, the larger the virtual soil's particles, the fewer the particles needed to simulate the virtual soil in our future simulations, and thus the shorter the simulation run time. The following function was found to be adapted to solving our problem and was thus used in the algorithm

$$\phi_4(x) = 10\left(\frac{\pi}{2} - \arctan(r - 5)\right)$$

where r is expressed in micrometres and dimensionless. Thus, the mathematical formulation of our optimization problem is

$$\phi(x) = \begin{bmatrix}\phi_1(x)\\ \phi_2(x)\\ \phi_3(x)\\ \phi_4(x)\end{bmatrix} = 0 \tag{4}$$

This nonlinear system of equations is overdetermined; it has four equations but only three unknowns. Consequently, in general, no exact solution to x can be found. However, an optimum solution minimizing the overall error can be computed.

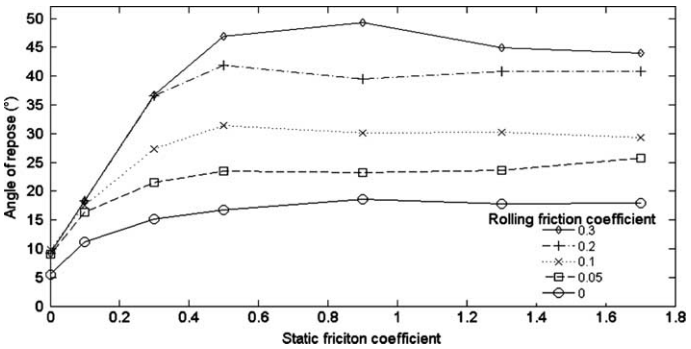

Figure 5. Angle of repose of the virtual soil for various friction coefficients, with $r = r_0 = 50\,\mu m$.

The Newton Gauss algorithm

To find this optimum solution, the Newton Gauss optimization algorithm was used (as described in Angeles, 2008)[2]. It finds the optimum design vector $x = (r, \mu_s, \mu_r)$ that minimizes the weighted least-squares error of the system of equations (4). In other words, it minimizes the function f defined as $f(x) = \frac{1}{2}\phi^T \mathbf{w}\,\phi$, with $\mathbf{W}$ being a 4×4 positive definite weighting matrix. To assign an identical weight to each ϕ_i function, the weighting matrix must be proportional to the identity matrix $\mathbf{W} = 0.25\mathbf{I}_4$ (in general, the sum of the weighting factors equals 1). The iterative algorithm starts from an initial guess, x^0. Then an increment, Δx^k, is iteratively added to the solution vector,

[2]J. Angeles. 2008. MECH 577 Optimum design (lecture notes). McGill University, Montréal, Quebec

x^k, until the convergence criterion $\|\Delta x^k\| \leq \varepsilon$ is reached: $x^{k+1} = x^k + \Delta x^k$. The increment Δx^k is computed as follows: $\Delta x^k = -\left(\Phi^{\mathrm{T}}\mathbf{w}\,\Phi\right)^{-1}\Phi^{\mathrm{T}}\mathbf{w}\,\phi$, in which Φ F is the 4×3 Jacobian of ϕ: $\Phi(x) = \frac{\partial\phi(x)}{\partial x}$. When the algorithm converges, the solution found is a local minimum but not necessarily the global minimum on the design space. Numerous initial guesses (x^0) were tried and converged to the same solution, which was then assumed to be a global optimum.

Results

For the silica Barco sand, the algorithm gave a satisfactory result. With equal weighting factors and a convergence criterion of $\varepsilon = 0.001$, it converged after 81 iterations to the solution $x = (r, \mu_s, \mu_r) = (70.85\ \mu\text{m}, 0.609, 0.0811)$. The estimated properties of the virtual soil were then $c = 23.9$ Pa, $\varphi = 29.5^\circ$, $A = 27.8^\circ$, whereas the measured values for the real soil were $c = 24$ Pa, $\varphi = 26.6^\circ$, $A = 30^\circ$ (cf. **Table 1**).

On the other hand, the algorithm did not converge in the case of the regolith (objective properties: $c = 0.3$ kPa, $\varphi = 40^\circ$, $A = 65^\circ$; property of the virtual soil: $c = 0.621$ kPa, $\varphi = 31.2^\circ$, $A = 36.7^\circ$ with the solution $x = (r, \mu_s, \mu_r) = (66.21\ \mu\text{m}, 1.44, 0.150)$). One reason for this could be the very high angle of repose of the regolith. As our simulations never showed an angle of repose greater than 50° (cf. **Figure 5**), the response surface of the virtual soil never reached $A = 65^\circ$ in the region of the design space that was explored. Reaching a greater angle of repose would require further investigation of the parameters' design space or the particle-prototype design. Decreasing the weighting factor of the objective function ϕ_1 (responsible for the angle-of-repose fit) to one-tenth of the other ones gave a better approximation: $c = 0.359$k, $\varphi = 38.7^\circ$, $A = 32.9^\circ$ with $x = (r, \mu_s, \mu_r) = (172.7\ \mu\text{m}, 1.21, 0.136)$.

Conclusion

This study presents a methodology for DEM parameter calibration of a virtual soil, involving geotechnical experiments on the real material and their simulations with DEM software. The example given in this paper shows how a virtual granular material can be calibrated to replicate the behaviour of a silica sand. However, lunar regolith behaviour could not be modelled accurately, probably because of a mediocre angle-of-repose surrogate model combined with a lack of design-space exploration.

This methodology could be greatly improved by better surrogate-model management. Indeed, an automated exploration of the design space in potentially optimum zones during the optimization process, which would allow an automated update of the response surfaces, would ensure high-fidelity surrogate models. Such an automated process was not possible with the current DEM software release, but can definitely be explored in future work.

Acknowledgements

The authors are grateful to Neptec, the Canadian Space Agency, and the Natural Sciences and Engineering Research Council's Collaborative Research and Development program for financial support of this project, and to DEM Solutions for the EDEM license and support.

References

Bekker, M.G. 2008. *Theory of land locomotion*. The University of Michigan Press, Ann Arbor, Mich.

Briend, R. 2010. *Modelling wheel–soil interactions using the discrete element method for tread shape optimization*. M.Sc. thesis, McGill University, Montreal, Que.

Coetzee, C., and Els, D. 2009. Calibration of discrete element parameters and the modelling of silo discharge and bucket filling. *Computers and Electronics in Agriculture*, Vol. 65, pp. 198–212.

EDEM. 2009. 2.1.1 *User guide*. DEM Solutions.

Heiken, G. 1991. *Lunar sourcebook: a user's guide to the moon*. Cambridge University Press.

Ji, S., and Shen, H. 2009. Two-dimensional simulation of the angle of repose for a particle system with electrostatic charge under lunar and earth gravity. *Journal of Aerospace Engineering*, Vol. 22, pp. 10–14.

Mindlin, R.D. 1949. Compliance of elastic bodies in contact. *Journal of Applied Mechanics*, Vol. 16, pp. 259–268.

Myers, R.H., and Montgomery, D.C. 2002. *Response surface methodology*. 2nd ed. John Wiley and Sons.

Tanaka, T., Tsuji, Y., and Ishida, T. 1992. Lagrangian numerical simulation of plug ow of cohesionless particles in a horizontal pipe. *Powder Technology*, Vol. 71, pp. 239–250.